

Thermal analysis and an improved heat-dissipation structure design for an AlGaInP-LED micro-array device*

TIAN Chao (田超)^{1,2}, GUO Shu-xu (郭树旭)¹, LIANG Jing-qiu (梁静秋)³, LIANG Zhong-zhu (梁中燾)³, and GAO Feng-li (郜峰利)^{1**}

1. State Key Laboratory on Integrated Optoelectronics, College of Electronic Science and Engineering, Jilin University, Changchun 130012, China

2. Semiconductor Manufacturing North China (Beijing) Corporation, Beijing 100176, China

3. Changchun Institute of Optics, Fine Mechanics and Physics, Chinese Academy of Sciences, Changchun 130033, China

(Received 1 March 2017; Revised 12 May 2017)

©Tianjin University of Technology and Springer-Verlag Berlin Heidelberg 2017

This paper describes a novel finite element thermal analysis model for an AlGaInP-LED micro-array device. We also conduct a transient analysis for the internal temperature field distribution of a 5×5 array device when a 3×3 unit is driven by pulse current. In addition, for broader applications, a simplified thermal analysis model is introduced and its accuracy is verified. The internal temperature field distribution of 100×100 units is calculated using the simplified model. The temperature at the device center reaches 360.6 °C after 1.5 s. In order to solve the heat dissipation problem of the device, an optimized heat dissipation structure is designed, and the effects of the number and size of the heat dissipation fins on the thermal characteristics of the device are analyzed.

Document code: A **Article ID:** 1673-1905(2017)04-0282-5

DOI 10.1007/s11801-017-7048-z

The AlGaInP-LED micro-array device with ultra high resolution has become the focus of research in recent years. However, many factors, such as unit arrangement, unit structure, device materials, and the fabrication process, will affect its thermal characteristics^[1-4]. Normally, the LED micro-array devices are still at the experimental stage and no mature product is available on the market^[5-7]. Thermal characteristic analyses of LED arrays are mainly carried out for single LEDs and arrays of these, while thermal characteristic analyses of LED micro-arrays are rare^[8-10]. A good understanding of the thermal behavior of AlGaInP-LED micro-array devices is important for both device structure optimization and fabrication process improvement^[11-14].

This paper introduces a novel three-dimensional finite element model for an AlGaInP-LED micro-array device. We also calculate and analyze the temperature distributions of AlGaInP-LED micro-array devices in different working conditions. We design an optimized heat dissipation structure that can significantly improve the temperature distribution in LED micro-array devices. It also permits control of the steady-state temperature in a practical range during device operation.

During the operation of LED micro-array devices, the internal temperature distribution follows the differential

equation for heat conduction:

$$\frac{\partial}{\partial x} \left(K_x \frac{\partial T}{\partial x} \right) + \frac{\partial}{\partial y} \left(K_y \frac{\partial T}{\partial y} \right) + \frac{\partial}{\partial z} \left(K_z \frac{\partial T}{\partial z} \right) + qv = \rho c \frac{\partial T}{\partial t}. \quad (1)$$

It is based on energy conservation and the Fourier law. Here, qv is the thermal power density, T is the transient temperature field, K_x , K_y , K_z are the thermal conductivities in three directions, respectively, ρ is the material density, and c is the specific heat of the material^[15-17].

Both additional boundary conditions and initial conditions are necessary to find the unique solution for the heat conduction differential equation^[18,19]. Considering the heat transfer between the fluid and the solid, and assuming that the temperature of the fluid medium T_f and the heat transfer coefficient α between them are known, the equation can be written as

$$-\frac{\partial}{\partial n} \Big|_r = \alpha(T - T_f) \Big|_r. \quad (2)$$

In addition, the temperature distribution for the object at any moment is determined, and the initial condition for the general temperature field is expressed as

$$T|_{t=0} = \varphi, \quad (3)$$

where φ is a known function that describes the temperature distribution for the object at the initial moment.

* This work has been supported by the Young Scientists Fund of the National Natural Science Foundation of China (No.61204055).

** E-mail: gaofl@jlu.edu.cn

According to the differential equation for heat conduction, the temperature field distribution is related to the specific heat, the heat transfer coefficient, and the density of the material. This assumes that the boundary conditions and the thermal power density are known^[20]. The 3×3 AlGaInP-LED micro-array structure is shown in Fig.1.

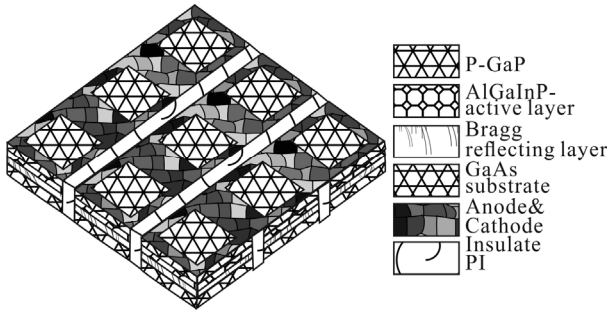


Fig.1 AlGaInP-LED micro-array structure

The thickness of the array device is 100 μm , the period of the array unit is 100 μm , and the size of the light-emitting unit is 80 $\mu\text{m} \times 80 \mu\text{m}$. Adjacent units are separated by polyimide with spacing of 20 μm . The light-emitting units of each row share the same anode, while the light-emitting units of each column share the same cathode. The shape of the anode electrode is the loop type to ensure a light emitting area large enough and current uniformity.

Considering a flat wall with a thickness of L , surface area of A , and thermal conductivity of K , the thermal resistance is expressed as

$$R_{\text{cond}} = \frac{L}{KA}. \quad (4)$$

As for the structure shown in Fig.2, the volume of the light-emitting unit is $V=10^{-12} \text{ m}^3$. Considering the layers of different materials, the thermal resistance relationship of the unit structure can be divided into a lateral equivalent thermal resistance network^[17,21]. This can be regarded as a GaP layer, an AlGaInP layer, and a GaAs layer in parallel, which is linked with PI layer in series and then linked with the electrode layer in parallel.

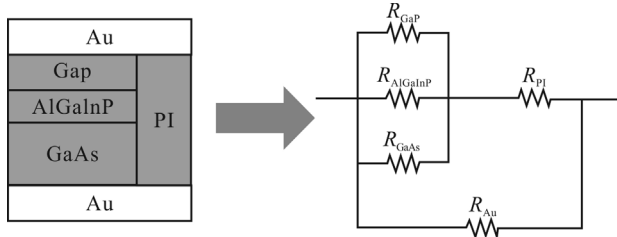


Fig.2 Thermal resistance model of the light-emitting unit

According to Eq.(4), the thermal resistance of each layer is calculated and listed in Tab.1.

Tab.1 Heat resistances of different layers

Material	Au	GaP	AlGaInP	GaAs	PI
Thermal resistance (K/W)	2.09×10^3	1.8×10^3	4.36×10^4	2.42×10^2	8.3×10^3

According to Tab.1, the total thermal resistance of a unit is

$$R_{\text{total}} = \frac{1}{\frac{1}{R_{\text{GaP}}} + \frac{1}{R_{\text{AlGaInP}}} + R_{\text{PI}}} + \frac{1}{R_{\text{Au}}} = 10.2 \times 10^3 \text{ (K/W)}. \quad (5)$$

Transient analysis is carried out for the temperature distribution of 3×3 light-emitting units located at the center of the array, which is driven by a pulse current of 50 Hz, 0.6 mA, as shown in Fig.3.

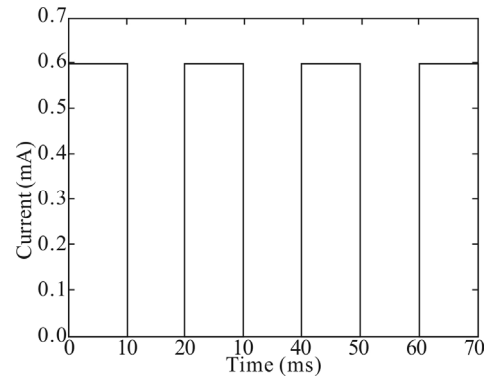


Fig.3 Pulse current

The path P (shown in Fig.4) between point A ($x=-24 \mu\text{m}$, $y=0 \mu\text{m}$, $z=92 \mu\text{m}$) and point B ($x=24 \mu\text{m}$, $y=0 \mu\text{m}$, $z=92 \mu\text{m}$) is created to obtain the temperature distribution for the active layer in x -direction.

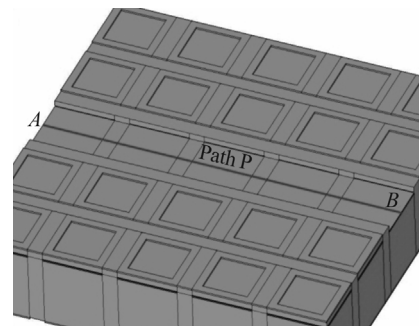


Fig.4 Schematic diagram of path P

Fig.5 shows the temperature distribution curves for 1.97 s, 1.98 s, 1.99 s and 2.00 s along the path P during the 3×3 unit operation. When several units work at the same time, the peak of the temperature distribution curve appears in the middle due to heat overlap.

Fig.6 shows the temperature variation in the center of the active layer inside the central unit. The temperature oscillates and increases with time, and it reaches the maximum (112.1 $^{\circ}\text{C}$) after 2.00 s operation. The heat

generated by the 3×3 unit operation is 9 times of that generated by a single unit. Without considering the heat dissipation and heat transfer away from the 5×5 array, through Eq.(6), the average temperature rise of $\Delta T = 202.5^\circ\text{C}$ is obtained after 2.00 s. When the heat dissipation and heat transfer away from the 5×5 array are taken into account, the actual temperature is smaller than this value. The maximum observed temperature rise for the array is 92.1°C at 2.00 s, which is less than ΔT . This validates the calculated results.

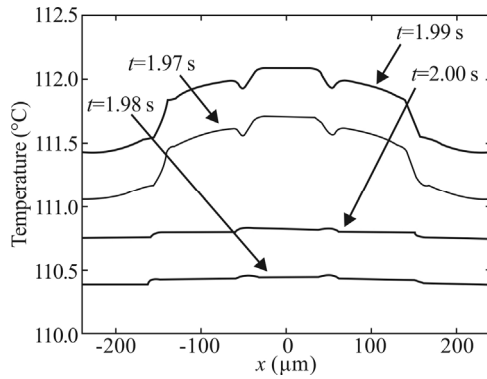


Fig.5 Temperature distribution curves at different time

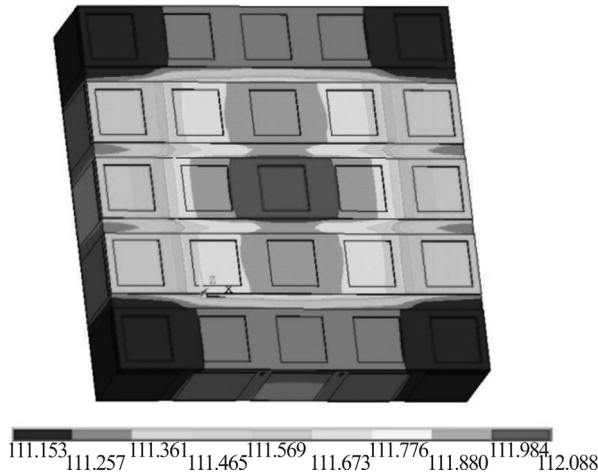


Fig.6 Temperature distribution at 1.99 s

Since the number of pixels is large in the array and the structure is complex, the finite element division, computing time and computer configuration are limited. It is difficult to build a model and calculate it in full accordance with the actual physical structure due to the large calculation power needed. Thus, it is necessary to simplify the calculation model.

Taking the small thickness of the device into account, the temperature distribution in the vertical direction can be neglected, and the temperature distribution on the surface of the device becomes the focus of the study. As for large size devices and a large number of units, when the structural size of the unit is much smaller than the overall size of the device, the unit structure of the device

has little effect on the temperature distribution of the whole device. Through the calculated thermal parameters, the device of the original model can be simplified to a flat plate whose thickness is $100\ \mu\text{m}$, which has no internal structure. The initial model and simplified model are shown in Fig.7 (when the operating time is 1.5 s).

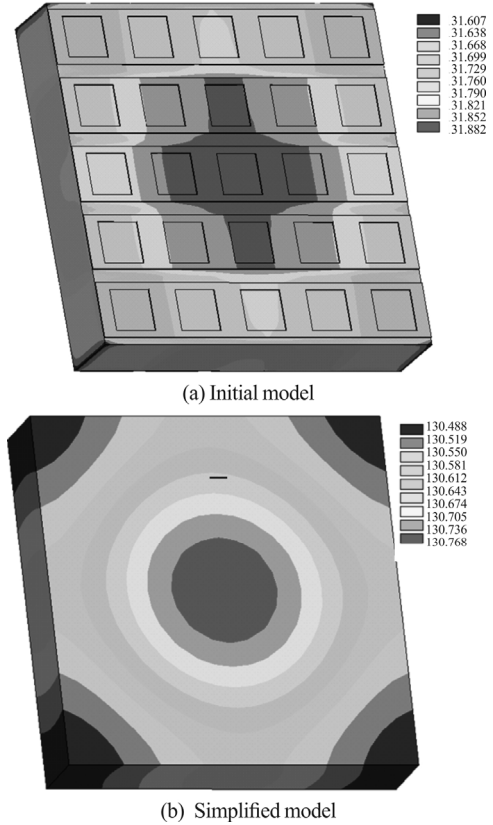


Fig.7 Temperature distributions of two models at 1.5 s

Furthermore, the array unit is regarded to be composed of the same material, and the average thermal parameters of the material are calculated using Eqs.(6)—(9). The average heat-transfer coefficient of the unit is

$$K_{\text{ave}} = \frac{L}{R_{\text{cond}} A} = 5.95 \text{ (W/m)}, \quad (6)$$

with the unit mass of

$$m = \sum_i V_i \rho_i = 4.62 \times 10^{-9} \text{ (kg)}, \quad (7)$$

where i is the material number, and V_i and ρ_i are the volume and density of the material, respectively. The density is

$$\rho = \frac{m}{V} = 4.62 \times 10^3 \text{ (kg/m}^3\text{)}. \quad (8)$$

The average specific heat is

$$c = \frac{\sum_i c_i m_i}{m} = 480.2 \text{ (J/kg} \cdot \text{K)}. \quad (9)$$

Device heat radiation is neglected in the calculation. The device is naturally cooled via the air through the

outer surface. The convection coefficient is set as $10 \text{ W/m}^2\cdot\text{K}$ and the air temperature is 20°C . It is assumed that the convection coefficient does not change with temperature. At a voltage of 2 V and a current of 0.6 mA , and considering that 20% energy of the LED is usually converted into light while the rest is converted into heat^[21], the thermal power of the device is about 1 mW . The formula to calculate the thermal power density is

$$H = \frac{P}{V}, \quad (10)$$

where H is the thermal power density, P is the thermal power, and V is the unit volume. According to the calculation, the power density of the heat source is set as $1 \times 10^9 \text{ W/m}^3$.

Fig.8 shows the time-varying curves for the central unit temperature based on two models. It shows the variation of temperature with time, and the two curves are similar to each other. At 1.5 s , the temperature of the original model is 131.9°C , while that of the simplified model is 130.8°C , so the relative error is 0.8% .

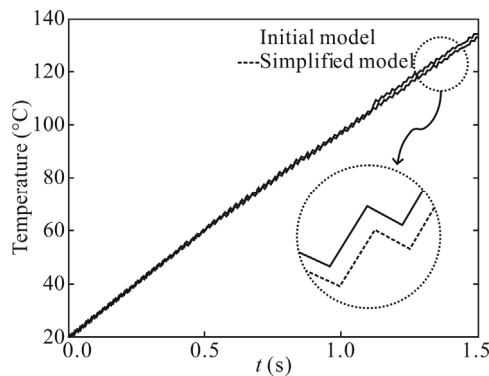


Fig.8 Time-varying curves of the central unit temperature for the two models

Fig.9 is the temperature distribution in the middle row. The two temperature distribution curves maintain the same trend of variation, and the temperature difference between two models at each position is always about 1°C .

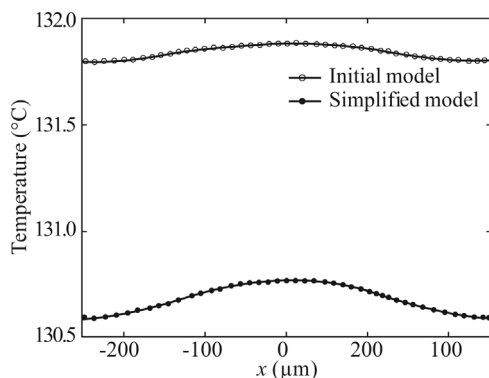


Fig.9 Temperature distributions in the middle row

Generally, the normal operating temperature of the

LED micro-array device is below 60°C . Under the condition of larger device size and low temperature, the difference between the two models will be smaller. Hence, this simplified model and the original model for the 5×5 array have almost the same temperature distribution. Therefore, it is possible to calculate the temperature distribution of large devices with many pixels by using the simplified model instead of the original one.

According to the above mentioned study, a simplified model for a micro-array device that includes 100×100 light-emitting units with the dimension of $10 \text{ mm} \times 10 \text{ mm} \times 100 \mu\text{m}$ is investigated. Fig.10 shows the relationship between the temperature at the device center and time, as well as the device temperature distribution for the array after 1.5 s . Due to the high device power, the temperature rises rapidly, and at the device center it reaches 360.6°C after 1.5 s . Through the above analysis and calculation, we find that in order to ensure long-time stable device operation, it is necessary to implement a heat dissipation structure in micro-array devices.

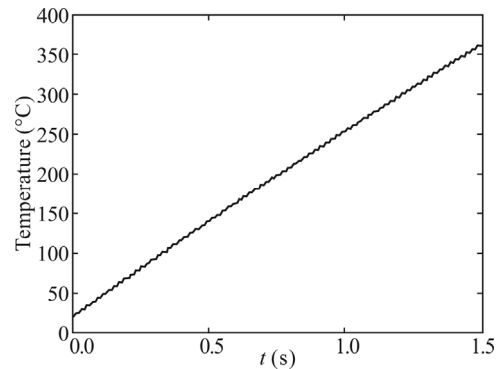


Fig.10 The relationship between the temperature at the device center and time

Here, a novel fin-type heat-dissipation structure is investigated. The material of the radiator is Cu, and the heat dissipation method is based on natural convection. The temperature field for the micro-array chip with the heat dissipation structure is calculated for 10 000 light-emitting units with 10 W power and the dimension of $10 \text{ mm} \times 10 \text{ mm} \times 100 \mu\text{m}$. The heat-dissipation structure is shown in Fig.11. The cross section radius is 30 mm , the thickness of the substrate is 5 mm , and the fin-thickness is 1 mm .

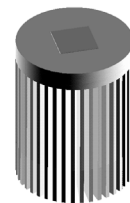


Fig.11 Schematic of the proposed heat-dissipation structure

The radiator structure should be optimized by increasing

the fin dimensions and quantity to enlarge the cooling area. This improves the heat exchange with the air. Fig.12 shows the variation of the maximum temperature of the chip for the radiator fins in steady-state condition. It shows that with the increase of the number of fins, the cooling area increases and the chip temperature decreases significantly. However, the declining trend slows down gradually. This means the enhancement of the chip cooling capacity is lower when the number of fins increases further. In addition, too many fins will lead to a small fin-spacing, which is not conducive to air flow and results in a cooling capacity decrease.

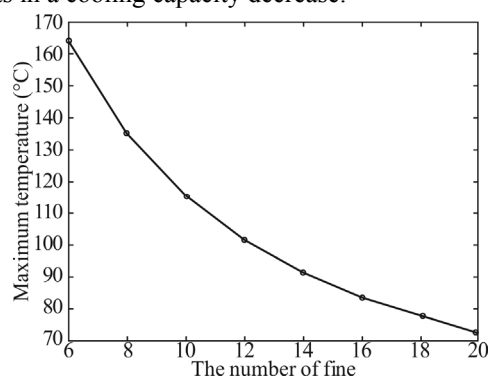


Fig.12 Maximum temperature vs. number of fins

Fig.13 shows the change of the maximum temperature on the chip with the height of the radiator in steady state, when the fins number is fixed to 20. It can be seen that the chip temperature decreases significantly after increasing the radiator height, but the declining trend slows gradually.

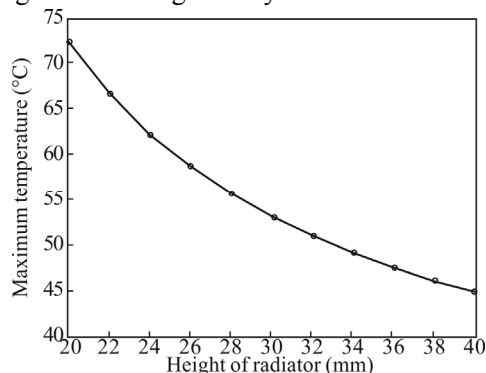


Fig.13 Maximum temperature vs. height of radiator

Increasing the cooling area of the radiator requires both above-mentioned methods at the same time. Furthermore, both size and weight of the radiator, as well as the steady-state distribution of the chip temperature, need to be considered. The optimized structure parameters for the heat-dissipation structure are 20 fins and a height of 40 mm, and we can decrease the device operating temperature from 360.6 °C to 45 °C.

In this paper, a new thermal model for an Al-GaN-LED array device is described, which uses finite element analysis. Transient analysis is carried out for a temperature distribution of 3×3 light-emitting units lo-

cated at the center of a 5×5 array device. A simplified model is established which is suitable for large-size multiple-pixel LED micro-arrays. After verification, we find that the simplified model yields almost the same temperature distribution as the original model. The relative error is only 0.8%. The temperature distribution for a 100×100 array device is calculated using the simplified model. Furthermore, to better solve the problem of heat dissipation, a finned radiator with a circular structure is designed. The structure of the radiator has been optimized. The effects of fin quantity and dimensions on the device temperature distribution are analyzed.

References

- [1] Gessmarn T and Schubert E F, *J. Appl. Phys.* **95**, 2203 (2004).
- [2] Li G, Wang W, Yang W, Lin Y, Wang H and Lin Z, *Reports on Progress in Physics Physical Society* **79**, 056501 (2016).
- [3] Shervin S, Kim S-H, Asadirad M, Karpov SY, Zimina D and Ryou J-H, *ACS Photonics* **3**, 486 (2016).
- [4] Kim M S, Lee H K and Yu J S, *Semicond. Sci. Technol.* **28**, 2 (2013).
- [5] Horng R H, Wu B R, Weng C F, Ravadgar P, Wu T M, Wang S P, Yang J H, Chen Y M, Hsu T C, Liu A S and Wu D S, *Opt. Express* **21**, 19668 (2013).
- [6] Li X F, Budai J D, Liu F, Howe J Y, Zhang J H, Wang X J, Gu Z J, Sun C J, Meltzer R S and Pan Z W, *Light: Science & Applications* **2**, e50–1 (2013).
- [7] Pan J W and Tsai P J, *Applied Optics* **52**, 1358 (2013).
- [8] Lee ATL, Chen H, Tan S-C and Hui SYR, *IEEE Transactions on Power Electronics* **31**, 65 (2016).
- [9] Tao X and Yang B, *Journal of Power Electronics* **16**, 815 (2016).
- [10] Xu M, Mu Q, Xiao L, Zhou Q, Wang H and Ji Z, *Materials Express* **6**, 205 (2016).
- [11] Chang S J, Zeng X F, Shei S C and Li S, *IEEE J. Topics Quantum Electron* **49**, 846 (2013).
- [12] Lee H K, Kim M S and Yu J S, *Microelectronic Engineering* **104**, 29 (2013).
- [13] Li K H and Cheung Y F, *IEEE Photonics Technology Letters* **25**, 374 (2013).
- [14] Kim H, Cho J, Lee J W, Yoon S, Kim H, Sone C and Park Y, *Appl. Phys. Lett.* **90**, 063510 (2007).
- [15] Kim H, Lee J M, Huh C, Kim S W, Kim D J, Park S J and Hwang H, *Appl. Phys. Lett.* **77**, 1903 (2000).
- [16] Kim H, Park S J and Hwang H, *IEEE Trans. Electron Devices* **48**, 1065 (2001).
- [17] Chang S J, Kuo C H, Su Y K, Wu L W, Sheu J K, Wen T C, Lai W C, Chen J F and Tsai J M, *IEEE J. Sel. Topics Quantum Electron* **8**, 744 (2002).
- [18] Ryu H Y and Shim J I, *Opt. Express* **19**, 2886 (2011).
- [19] Tian P F, Jonathan J D M, Gong Z, Guilhabert B, Watson I M, Gu E, Chen Z Z, Zhang G Y and Dawson M D, *Appl. Phys. Lett.* **101**, 231110 (2012).
- [20] Tian C, Wang W B, Liang J Q, Liang Z Z, Qin Y X and Lv J G, *AIP Advance* **5**, 041309 (2015).
- [21] Dai Q, Shan Q F and Wang J, *Appl. Phys. Lett.* **97**, 133507 (2010).